Environmental Science & Technology

Article

pubs.acs.org/est

Rates of Hydroxyl Radical Production from Transition Metals and Quinones in a Surrogate Lung Fluid

Jessica G. Charrier[†] and Cort Anastasio*[,†]

[†]Department of Land, Air and Water Resources, University of California, Davis, 1 Shields Avenue, Davis, California 95616, United States

Supporting Information

ABSTRACT: Hydroxyl radical (•OH) is the most reactive, and perhaps most detrimental to health, of the reactive oxygen species. •OH production in lungs following inhalation of particulate matter (PM) can result from redox-active chemicals, including iron and copper, but the relative importance of these species is unknown. This work investigates •OH production from iron, copper, and quinones, both individually and in mixtures at atmospherically relevant concentrations. Iron, copper, and three of the four quinones (1,2-naphthoquinone, phenanthrenequinone and 1,4-naphthoquinone) produce •OH. Mixtures of copper or quinones with iron synergistically produce •OH at a rate 20−130% higher than the sum of the rates of the individual redox-active species. We developed a regression equation from 20 mixtures to predict the rate of •OH production from the particle composition. For typical PM compositions, iron and copper account for most •OH production, whereas quinones are a minor source, although they can contribute if present at very high concentrations. This work shows that Cu contributes significantly to •OH production in ambient PM; other work has shown that Cu appears to be the primary driver of HOOH production and dithiothreitol (DTT) loss in ambient PM extracts. Taken together, these results indicate that copper appears to be the most important individual contributor to direct oxidant production from inhaled PM.

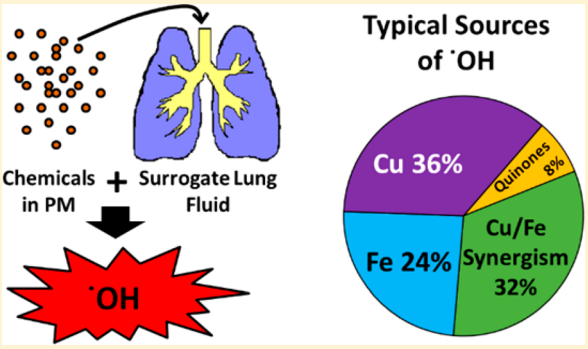

INTRODUCTION

Inhalation of ambient particulate matter (PM) can produce adverse health effects and mortality in humans,[1,2] which may be mediated through the ability of PM to produce reactive oxygen species (ROS).[3,4] An overproduction of ROS can overwhelm the body's antioxidant defenses, causing oxidative stress, inflammation, and disease.[5,6] Hydroxyl radical (•OH) is the most damaging of the ROS, reacting with most biological molecules, including DNA, at diffusion-controlled rates.[4,7−11] In fact, most of the toxicity associated with other ROS (e.g., superoxide or hydrogen peroxide) might be due to their ability to form •OH.[12]

•OH is formed by the well-known Fenton reaction involving reduced iron (Fe(II)) and hydrogen peroxide (HOOH):

$$\mathrm{Fe(II) + HOOH \rightarrow Fe(III) + {}^{\bullet}OH + {}^{-}OH} \quad \text{(R1)}$$

Other reduced transition metals, including Cu(I), Ti(III), Cr(III), Ni(II), Co(II), Pb(II), and Cd(II) can also form •OH through a Fenton-like reaction in the presence of HOOH.[13−16] In airborne particles Fe is the most abundant transition metal, typically followed by Cu; soluble concentrations of the other transition metals in PM are typically very low.[17] Background HOOH is produced by cells in the lungs, though the concentration is likely low.[18] However, trace levels of Fe and Cu can catalytically form •OH in the absence of initial HOOH if a reductant—such as ascorbate (vitamin C)—is present to cycle the metal back to its reduced state after it participates in the Fenton(-like) reaction.[19−21] Under these conditions both Fe and Cu can transfer electrons from ascorbate to dissolved molecular oxygen, forming superoxide, HOOH and •OH in series.

In addition to this metal chemistry, there is also evidence that redox-active quinones might be important for •OH production. Quinones produce HOOH in the presence of a reductant such as ascorbate or DTT.[22,23] In the presence of Fe this quinone-mediated production of HOOH accelerates the rate of the Fenton reaction and enhances •OH production.[24] Quinones can also reduce Fe(III) to Fe(II), increasing the rate of the Fenton reaction in the absence of a reductant;[25] however, ascorbate efficiently cycles Fe(III) to Fe(II) and Cu(II) to Cu(I) in our system,[19] so metal reduction by quinones is not likely important under these conditions. There are also recent reports of a direct mechanism of •OH production from quinones in the presence of ascorbate that does not include the Fenton reaction.[26,27]

Multiple studies have shown that ambient PM can chemically generate •OH in the presence of ascorbate.[20,28−30] Though

Received: March 30, 2015
Revised: June 27, 2015
Accepted: July 8, 2015
Published: July 8, 2015

DOI: 10.1021/acs.est.5b01606
Environ. Sci. Technol. 2015, 49, 9317−9325

both quinones and metals can contribute to •OH production from PM, it is not clear how important each class is to overall •OH formation, as no previous research has systematically studied both chemical classes under physiologically relevant conditions. Additionally, while the metal content of PM has long been associated with adverse health effects,[6,31−35] it is still unclear which metal or metal mixtures are most important for toxicity. We have previously reported the 24 h total •OH production from transition metals in a surrogate lung fluid[19] and investigated the rates of HOOH production from metals and quinones in the same reaction system.[22] Here we extend our previous •OH results to include redox-active quinones, and mixtures of Fe, Cu, and quinones. Instead of the 24 h total •OH amounts that we reported previously, in this work we measure the average rate of •OH production between 0 and 4 h. As we have done for DTT loss[17] and HOOH formation,[22] here we measure the •OH rates for individual and mixed metals and quinones to make it possible to quantify the contributions of these species to •OH production in ambient PM extracts. From our measurements we are able to derive a master equation to predict the rates of •OH production in ambient PM extracts based on the concentrations of soluble metals and quinones. This formula works well for ambient PM samples, the confirmation of which will be presented in future work.[36] Finally, using a typical PM composition we compare the relative importance of individual transition metals and quinones to •OH production, HOOH production,[22] and dithiothreitol (DTT) loss[17] to give a more holistic picture of the relative importance of each redox-active species in cell-free assays.

EXPERIMENTAL SECTION

Chemicals. Chemical forms and their purities are described in the Supporting Information section S1.

Surrogate Lung Fluid. The surrogate lung fluid (SLF) consists of phosphate-buffered saline (PBS), an •OH probe, and four added antioxidants.[19] The PBS contains 114 mM NaCl, 7.8 mM sodium phosphate dibasic, and 2.2 mM potassium phosphate monobasic to yield a pH of 7.2 to 7.4; 10 mM of sodium benzoate is added as a •OH probe. The PBS with benzoate is treated with Chelex 100 resin (Biorad) to remove trace metals; this crucial step is necessary to reduce background levels of transition metals in order to get the correct concentration−response relationships (as well as to properly measure oxidants or oxidative potential in ambient samples). Antioxidant stock solutions are made fresh each day and are added to the PBS-benzoate mixture just prior to the start of each reaction. Final concentrations in the SLF are 200 μM L ascorbic acid sodium salt (Asc), 300 μM citric acid (Cit), 100 μM reduced L-glutathione (GSH), and 100 μM uric acid sodium salt (UA).

Metal and Quinone Stocks. Copper(II) sulfate and iron(II) sulfate stocks were made from solid in ultrapure water (Milli-Q, 18.2 MΩ·cm) on the day of the experiment. Phenanthrenequinone (PQN), 1,2-naphthoquinone (1,2-NQN), 1,4-naphthoquinone (1,4-NQN), and 1,4-benzoquinone (BQN) stocks were made in acetonitrile in amber glass vials and were stored at −20 °C. Note that quinones are highly toxic, possible human carcinogens, and semivolatile so must be handled and stored with extreme caution. We monitor the concentration of quinone stocks over time using a UV/vis spectrophotometer (Shimadzu, UV-2501PC) and find the solutions are stable for over one year. Molar absorptivities can be found in Charrier et al.[22]

Quantification of •OH. We quantify •OH using a sodium benzoate probe technique described in detail in the literature.[19,30,37] Briefly, •OH is quantitatively trapped by sodium benzoate forming *p*-hydroxybenzoic acid (*p*-HBA) as a stable product. We quantify *p*-HBA using HPLC with UV/vis detection and daily calibration curves of *p*-HBA standards made in Chelex-treated PBS. The total concentration of •OH formed after a given time is calculated from the concentration of *p*-HBA in the sample. To calculate the rate of •OH formation (as opposed to the rates of *p*-HBA formation or •OH trapped), we use the yield of *p*-HBA from the •OH-benzoate reaction and the fraction of •OH that reacts with sodium benzoate (as opposed to other compounds in solution). Detailed information on this calculation is available in our previous publication.[19]

The antioxidants and transition metal or quinone stock solutions are made individually. We add SLF and rapidly mix the antioxidants and metal or quinone stocks to a final volume of 5.0 mL in acid-washed FEP bottles, record the reaction start time, cap and shake. Experiments are performed with room lights off and bottles are further shielded from light with aluminum foil. At 0, 1, 2, and 4 h we remove a 0.80 mL aliquot and immediately quench it with 16 μL of 5 mM desferoxamine (DSF) and 16 μL of 21 mM sodium bisulfite ($NaHSO_3$) to bind transition metals and destroy HOOH, giving a final concentration of 100 μM DSF and 400 μM sodium bisulfite. After allowing this mixture to react for at least 5.0 min, we add 19.2 μL of 0.5 M sulfuric acid to acidify the solution for HPLC analysis. Samples are stable for at least 18 h at room temperature in the dark.

We calculate the average rate of •OH production from zero to 4 h using the linear slope over that time period. In some cases initial •OH production has a slight lag (Supporting Information Figure S1), so data are not always strictly linear from zero to 4 h. Other authors have observed similar behavior for •OH production from dithiothreitol (DTT) and Cu.[38] Thus, the average rate reported here is not always equal to the instantaneous initial rate, which can sometimes be lower due to a lag in •OH production. While the production of •OH over 4 h is nearly always linear, •OH production over 24 h is not. Thus, our previous 24 h integrated •OH totals[19,21,30] cannot be used to calculate rates of •OH production (Supporting Information Figure S2). The rate of •OH production is necessary to understand the contributions to •OH production from individual and mixed redox-active species and to compare to our HOOH rate measurements made in the same solutions. Additional information can be found in Supporting Information section S3.

On each experiment day we also measure •OH production in a blank and a positive control (1.44 μM $FeSO_4$). All rates are blank-corrected by subtracting the blank rate from the reaction rate. The average ($\pm 1\sigma$) blank and blank-corrected positive control rates are 0.096 ± 0.04 (n = 14) and 0.97 ± 0.08 (n = 10) μM •OH/h, respectively.

Data Analysis and Statistics. Data are reported as the average ± one standard deviation, calculated from replicates. We used the statistical language R[39] to run multiple linear regressions on the mixture results.

DOI: 10.1021/acs.est.5b01606
Environ. Sci. Technol. 2015, 49, 9317−9325

RESULTS AND DISCUSSION

Rate of •OH Production from Individual Redox-Active Species. Based on our previous 24 h measurements of total •OH production from transition metals, Fe and Cu produce •OH in SLF, whereas the other eight metals we tested (Cd, Co, Cr, Mn, Ni, V, Zn, and Pb) cannot.[19] We started this work by measuring the rate of •OH production from 500 nM of Fe and Cu as well as four quinones (also at 500 nM) that have not been previously tested. These quinones—phenanthrenequinone (PQN), 1,4-benzoquinone (BQN), 1,2-naphthoquinone (1,2-NQN) and 1,4-naphthoquinone (1,4-NQN)—are some of the most frequently measured in atmospheric particles.[17] BQN did not produce •OH, whereas the other three quinones all produced •OH at a rate similar to that of Fe(II) and Cu(II) (Figure 1). While it is possible that the active quinones can

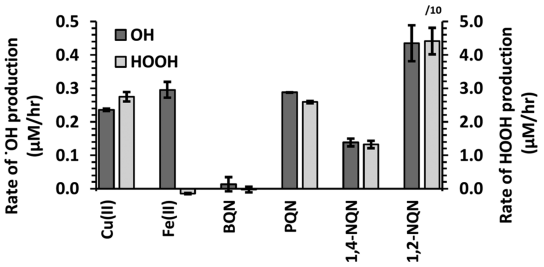

Figure 1. Rates of •OH and HOOH production from 500 nM of individual redox-active species. The error is the standard deviation of replicates ($n \geq 2$). HOOH rate data are from Charrier et al.;[22] Fe(II) destroys background HOOH, resulting in a slightly negative rate of HOOH production. Note that the 1,2-NQN rate of HOOH production and error bar are divided by 10 to fit on the scale.

produce •OH directly in the presence of Asc,[26] it is also possible that the quinones are only able to produce HOOH and that trace Fe (or Cu) converts the HOOH to •OH; we explore this idea further in the next section. As shown on the right-hand axis of Figure 1, Cu(II), PQN, and 1,4-NQN each produce HOOH[22] with a rate that is 10 times higher than their respective OH formation rate. In contrast, HOOH production by 1,2-NQN (which is divided by a factor of 10 in Figure 1) is 100 times faster than the rate of •OH production. Thus, for these redox-active species, approximately 1% (for 1,2-NQN) or 10% (for Cu, PQN, and 1,4-NQN) of the HOOH produced is converted to •OH in the initial 4 h. Fe(II), on the other hand, produces no measurable HOOH and, in fact, destroys background HOOH: The concentration of HOOH over time is less than the concentration at time zero, resulting in a negative rate of HOOH production (Figure 1). Since HOOH is a necessary reactant to form •OH, it is likely that Fe forms HOOH but that its concentration is maintained at a very low level because Fe rapidly converts HOOH into •OH via the Fenton reaction.[22] Though we used the reduced from of Fe (Fe^{+2}) and the oxidized form of Cu (Cu^{+2}), rapid redox cycling of the metals by Asc means the •OH rate should not depend on the initial metal oxidation state. A discussion of this point is in the Supporting Information Section S6.

Rates of •OH Formation as a Function of Species Concentration. Figure 2 shows the rate of •OH production from individual redox-active metals and quinones as a function of their concentration. Additional plots of these data, including the full concentration ranges for Fe and Cu, are in Supporting Information Figure S3. For Cu, •OH production initially

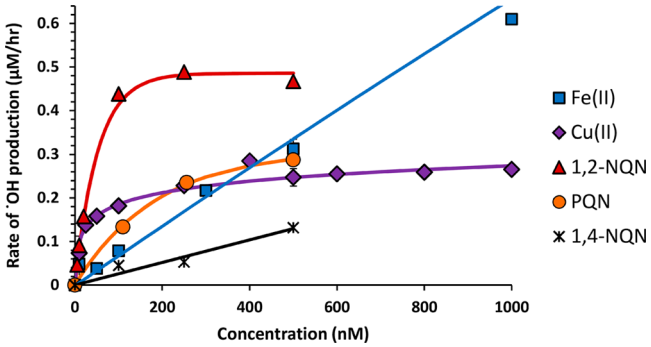

Figure 2. Rates of •OH production as a function of concentration of individual redox-active species. Equations for the regression lines are listed in Table 1.

increases rapidly with Cu concentration up to approximately 25 nM, increases much more slowly after that, and nearly plateaus after approximately 200 nM Cu. 1,2-NQN, and PQN show similar behavior, whereas 1,4-NQN exhibits a linear concentration response between 0 and 500 nM. The Fe concentration response is linear across a large Fe concentration range, but begins to plateau around 8000 nM (Supporting Information Figure S3a). The equations for these concentration−response regressions are summarized in Table 1.

We believe Cu exhibits a nonlinear response because it rapidly destroys Asc, thus running out of the reductant needed to cycle Cu(II) to Cu(I). We can qualitatively identify ascorbate in our HPLC chromatograms, and observe rapid loss of the Asc peak within 2−4 h in the presence of Cu, but not with other species. Despite this evidence, it is possible that other factors, such as the kinetics of electron transfer from Asc to the redox-active species (or from the redox-active species to O_2, $^{\bullet}O_2^-$, or HOOH), are controlling the concentration−response curves in Figure 2 and Supporting Information Figure S3. Regardless of the mechanism, the nonlinear behavior of Cu has important consequences for •OH production. First, at Cu concentrations larger than about 200 nM, •OH production is nearly constant, and an increase in Cu concentration causes only a small increase in the amount of •OH produced. Second, because the rate of formation of •OH is not linear as a function of Cu concentration, the resulting rate will depend on how much PM is added to the assay since this determines the final Cu concentration in the extract. However, as we discuss later, the synergistic increase in •OH production from mixtures of Fe and Cu mitigates some of this behavior.

Supporting Information Figure S4 shows the rates of HOOH and •OH production as a function of redox-active species concentration. HOOH production from Cu is 10 times larger than •OH production across all concentrations tested and both the HOOH and •OH concentration−response curves show a similar shape (Supporting Information Figure S4a). This suggests that •OH production from Cu is tied to HOOH production. This is different than the 1,2-NQN and PQN data (Supplorting Information Figures S4b and S 4d respectively): these quinones show a linear increase in the rate of HOOH production with increasing quinone concentration but a weaker, nonlinear response for •OH, which increases with quinone concentration initially then plateaus at higher concentrations. Because HOOH does not plateau, and thus does not become limiting, this result suggests that something else limits the conversion of HOOH to •OH at higher concentrations. This result could be explained if trace Fe is

DOI: 10.1021/acs.est.5b01606
Environ. Sci. Technol. 2015, 49, 9317−9325

Table 1. Regression Equations for the Rate of •OH Production As a Function of Concentration of Individual and Mixed Redox-Active Species

equation number	compound(s)	regression[a]	R^2	concentration range (nM)[b]	number of data points
		Individual Compounds			
equation 1	Cu(II)	$R_{OH} = 0.0383 \times \mathrm{Ln}([\mathrm{Cu}]) + 0.009$	0.95	0.8[c] − 10 000	14
equation 2	Fe(II)	$R_{OH} = (-3.13 \times 10^{-8})[\mathrm{Fe}]^2 + (6.86 \times 10^{-4})[\mathrm{Fe}]$	0.995	0−10 000	13
equation 3	1,2-NQN	$R_{OH} = 0.486 \times (1\text{-}\exp(-0.0191 \times [1,2\text{-NQN}]))$	0.997	0−500	7
equation 4	1,4-NQN	$R_{OH} = (2.59 \times 10^{-4}) \times [1,4\text{-NQN}]$	0.94	0−500	4
equation 5	PQN	$R_{OH} = 0.312 \times (1\text{-}\exp(-0.0053 \times [\mathrm{PQN}]))$	0.999	0−500	4
		Mixtures of Fe, Cu, and/or Quinones			
equation 6	Mixture	$R_{OH} = 0.198 \times (R_{HOOH,Cu} + 1.56 \times R_{HOOH,Q}) + 8.64 \times 10^{-4} \times [\mathrm{Fe(II)}]$	0.993	n/a	20
	Where	$R_{HOOH,Cu}$ is the rate of HOOH production from Cu in μM/h[d] $= 0.524 \times \ln([\mathrm{Cu}]) - 0.615$			
		$R_{HOOH,Q}$ is the sum of rates of HOOH from quinones in μM/h[d] $= 0.050 \times [1,2\text{-NQN}] + 0.0052 \times [\mathrm{PQN}] + 0.0024 \times [1,4\text{-NQN}]$			

[a] R_{OH} is the rate of •OH production in μM/h and [X] is the concentration of redox-active chemical species in nM. [b] Regression equations may not be valid outside of the concentration ranges measured. [c] The Cu(II) regression equation goes to zero at 0.8 nM of Cu(II). •OH values should be assumed to be zero at copper concentrations below this. [d] The rates of HOOH production from Cu and quinones in eq 6 are regression equations from individual species measured previously.[22]

responsible for converting HOOH to •OH: at low quinone concentrations the rate of HOOH production is limiting •OH formation, but at high quinone concentrations •OH production is limited by the trace Fe concentration. It is unclear why the 1,4-NQN data looks different than the other quinones—in this case both HOOH and OH formation rates are linearly dependent on quinone concentration—but it may be that the amount of HOOH produced is too little to reach a level where Fe becomes limiting.

Rates of •OH Production in Mixtures of Redox-Active Species. While •OH production from individual species is an important starting point, we are more interested in the behavior of mixtures of redox-active species that mimic extracts of ambient PM. In Figure 3 we measure the rate of •OH production from simple mixtures of Fe, Cu, and/or quinones (individual gray bars) and compare it to the sum of •OH production rates from individual species at the same concentrations used in the mixture (colored stacked bars). As shown in the left pair of bars, a mixture of Cu and PQN produces a rate of •OH that is very similar to the sum of rates from the individual species, indicating no interaction between the species. This agrees with our previous measurements of the rate of HOOH production: mixtures of Cu with either PQN or 1,2-NQN produce the same amount of HOOH as the sum of individual species.[22]

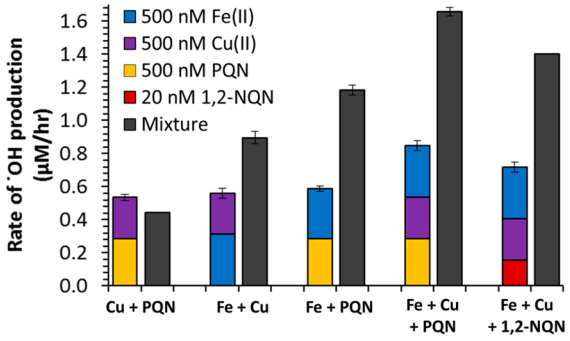

Figure 3. Rate of •OH production measured in a mixture (right gray bar) and calculated as the sum from individual species (left stacked bar). The difference within each pair of bars represents the synergistic •OH production from Fe. Errors on gray bars are the standard deviation of replicate measurements, while errors on colored bars are the propagated error of replicate measurements for each species in the bar.

We have previously shown that adding Fe to solutions containing Cu and/or quinones substantially suppresses the rate of HOOH production,[22] but that mixtures of Fe and Cu synergistically produce more •OH over 24 h.[19] In Figure 3, we confirm that all mixtures of Cu with Fe synergistically produce •OH at a rate faster than expected from the individual species. The mixture of 500 nM Fe and 500 nM Cu produces 60% more •OH than expected from the individual solutions, broadly consistent with our 24 h result.[19] In the case of 500 nM Fe and 500 nM PQN, the rate of •OH production in the mixture is twice that expected from adding the rates from the individual species, confirming that the Fe-mediated enhancement in •OH is not limited to Cu, but also extends to other species that make HOOH. As shown in the final two sets of bars in Figure 3, ternary mixtures of Fe, Cu and either PQN or 1,2-NQN also show synergistic behavior, with nearly a 2-fold enhancement in the rate of •OH formation.

To further investigate this effect we measured •OH production from additional mixtures containing Fe, Cu, and/or quinones across multiple concentration ranges (Supporting Information Table S1). Eight of the mixtures represent the concentrations of Fe, Cu, and quinones we measured in individual ambient PM extracts (data not yet published), representing realistic PM compositions. All 20 mixtures produced •OH at a faster rate than predicted from the individual species, with enhancements of 19 to 131% (Supporting Information Table S1). Based on these results, we hypothesized that synergistic •OH production is related to the Fenton reaction R1. Cu and quinones form HOOH efficiently while Fe cannot efficiently form HOOH, but can convert HOOH to •OH. If the rate of •OH production from Fe individually is limited by the availability of HOOH (as indicated by complete conversion of HOOH to •OH in Fe solutions) then the addition of Cu and quinones will increase the available HOOH and allow Fe to convert a portion of that HOOH to •OH. This results in a decrease in the rate of HOOH formation as compared to Cu and quinones individually and an increase in the rate of •OH formation.

DOI: 10.1021/acs.est.5b01606
Environ. Sci. Technol. 2015, 49, 9317−9325

Using this hypothesis we calculated a regression equation (eq 6) that can predict the rate of •OH production based on the rates of HOOH formation by individual species and the concentration of Fe (Table 1). In this equation the rate of HOOH production is calculated from concentration−response curves of copper and quinones,[22] allowing us to predict •OH production in mixtures based just on the concentrations of Fe, Cu, and quinones. All regression coefficients in eq 6 are statistically significant ($p < 0.05$) and the R^2 is 0.993. As shown in Figure 4, eq 6 accurately explains •OH production in our 20

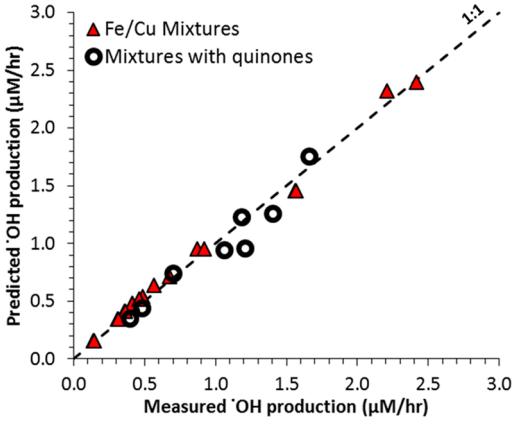

Figure 4. Measured versus predicted rates of •OH production from mixtures of Fe, Cu, and/or quinones. The predicted •OH is calculated using eq 6 in Table 1. This equation works for mixtures of Fe and Cu (triangles) and mixtures of Fe and/or Cu and quinones (circles). The composition of all solutions is included in the Supporting Information Table S1.

mixtures for solutions that contain Fe and Cu, Fe and quinones, and mixtures of all three species. Most mixtures show excellent agreement between measured and predicted values, and only a few quinone mixtures fall just below the 1:1 line. The linear regressions of measured versus predicted •OH production is excellent both for the subset of Fe/Cu mixtures (slope ±1 SE = 0.97 ± 0.02; R^2 = 0.99) and for the subset of mixtures containing metals and quinones (slope = 1.0 ± 0.1; R^2 = 0.93). In separate work we have also applied this regression to samples of ambient particulate matter and find good agreement between the measured •OH rate and that predicted by eq 6.[36]

The fitted regression equation treats HOOH production from Cu and quinones differently, indicating a slightly different mechanism of •OH production. The coefficient of 1.56 before the rate of HOOH formation from quinones ($R_{HOOH,Q}$) in eq 6 indicates that HOOH from quinones forms •OH more efficiently than HOOH from Cu, suggesting a secondary mechanism in mixtures. Quinones or quinone-metal mixtures may enhance the production of •OH or mixtures of Fe and Cu may suppress the formation of •OH. We investigate this question by comparing the impacts of Fe on the both the suppression in HOOH and the enhancement in •OH for a mixture with the same composition of Fe, Cu and quinones. We calculate HOOH suppression as the difference in rate for a solution containing only Cu and a solution containing the same concentration of Cu mixed with Fe. For example, the measured rate of HOOH production from 1 μM Cu minus the measured rate of HOOH production from 1 μM Cu mixed with 1 μM Fe gives the absolute decrease in HOOH production upon Fe addition. •OH enhancement is calculated as the rate of •OH production in the mixture with Fe minus the •OH rate in the same mixture without Fe; for example, this is the difference between the dark gray and stacked colored bars in Figure 3. If the Fenton reaction R1 explains the impacts of Fe addition, then the suppression in HOOH would equal the enhancement in •OH. However, as shown in Figure 5, this is only true in two

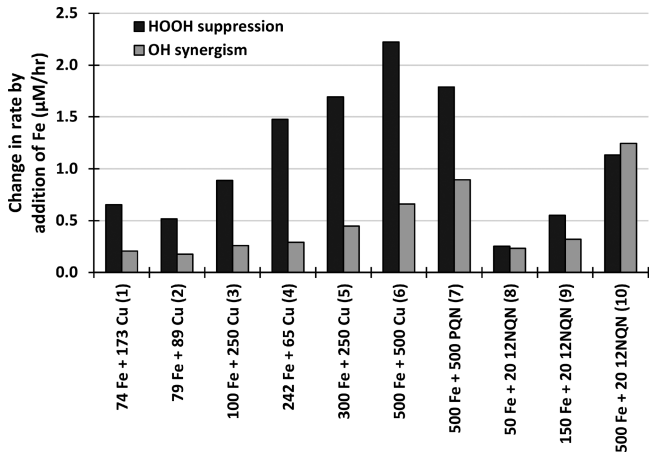

Figure 5. Suppression in the rate of HOOH formation, and corresponding enhancement in the rate of •OH formation, when Fe is added to a solution. The change in each HOOH rate is negative (i.e., adding Fe suppresses HOOH formation), but is plotted here as the absolute value. Each *x*-axis label indicates the composition of the solution and the concentration (in nM) of each metal and/or quinone. HOOH data are from Charrier et al.[22]

out of eight samples. In mixtures of Fe and Cu (solutions 1−6 in Figure 5) the enhancement in the •OH is only 20−34% of the corresponding suppression in the HOOH, indicating that Fe acting via the Fenton reaction can only explain a small portion of the HOOH suppression. Adding Fe to quinone solutions (solutions 7−10 in Figure 5) results in a closer match between HOOH suppression and •OH enhancement, suggesting a larger role for Fenton chemistry. In solutions 7 and 9, the •OH rate enhancement is 50 and 58%, respectively, of the corresponding suppression in HOOH, while in solutions 8 and 10 the enhancement in the OH rate is essentially equal to the corresponding suppression in the HOOH rate. Thus, while the results of solutions 8 and 10 are consistent with Fe stoichiometrically converting HOOH to OH via R1, for the other eight mixtures it appears that the addition of Fe causes a reduction in the initial rate of HOOH production. The more efficient Fe-mediated conversion of HOOH to OH in solutions of quinones (compared to solutions containing Cu) in Figure 5 is also consistent with regression eq 6, which indicates that HOOH from quinones more efficiently forms •OH than HOOH from Cu.

Implications for •OH Production from Ambient PM. We next use our concentration−response and mixture results from above, in conjunction with typical ambient concentrations of metals and quinones from the literature, to identify the relative importance of these redox-active species for •OH production in ambient PM extracts. While there are other redox-active species in atmospheric particles, such as humic-like substances,[40] not enough is known about their responses in the ROS assays to account for them in our calculations. We previously reported the ranges of soluble metals and particulate quinones summarized from the literature and the expected

DOI: 10.1021/acs.est.5b01606
Environ. Sci. Technol. 2015, 49, 9317−9325

ranges of HOOH production rates from individual redox-active species[22] (reproduced in Supporting Information Table S2). Using this same composition data we consider three cases for •OH: (1) "low" using the minimum reported concentration of each redox-active species, (2) "median" using the median concentration of each species, and (3) "high" using the maximum concentration of each species (Supporting Information Table S2). While these three example cases account for the range of concentrations reported in the literature, the actual contribution to •OH production for a specific particle sample will depend on its composition.

Figure 6 summarizes the relative •OH contribution from each species, including the synergistic contributions from Fe/

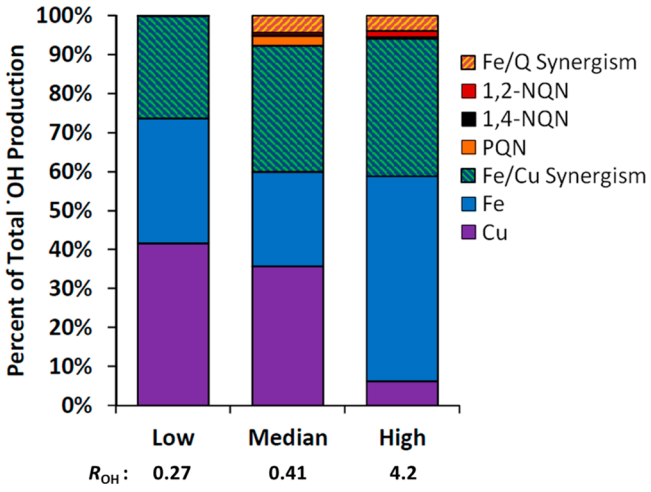

Figure 6. Contributions from individual species, and synergistic effects with Fe, toward •OH production for three hypothetical extracts of ambient PM using low, median, and high concentrations of particulate redox-active species reported in the literature (Supporting Information Table S2). Data are displayed as a percentage of the total rate, with the absolute rate (R_{OH}) listed below in units of μM/h.

Cu and Fe/quinone interactions. To determine the synergistic contributions we calculate the total rate of •OH production using eq 6, then calculate the rate for Fe and Cu using the same equation, but excluding the $HOOH_Q$ term. The difference between these two calculations gives the total •OH production by quinones. We then calculate the expected •OH production from individual quinones from eqs 3−5. The difference between this and the total production by quinones provides the synergistic production by quinones and Fe. Similarly we calculate the individual and synergistic contribution of Fe and Cu by subtracting the contributions from Cu and Fe individually and the total quinone contribution from •OH production.

Soluble Cu and Fe are most important to •OH production, although their relative contributions vary in the three different scenarios (Figure 6). Individually, Cu contributes 6−44% of total •OH, Fe contributes 24−53% and quinones contribute 0−3%; quinones account for a very small portion because their ambient particulate concentrations are low. Synergism between Fe and Cu is also important, accounting for 26−36% of •OH production while Fe-quinone synergy accounts for only 0.08% - 4% of total •OH production. Synergistic effects increase the total rate of •OH production by 35%, 52%, and 60% in the low, median and high cases.

The relative contribution by Cu goes down as concentrations increase from the low to high case, while the relative importance of Fe goes up with increasing concentrations. This is due to the shapes of the •OH concentration response curves (Figure 2): Cu plateaus at very low Cu concentrations, while •OH production from Fe increases with increasing concentration until very high levels (around 8000 nM). Interestingly, whereas the relative importance of Fe and Cu change, the relative •OH production from the Fe/Cu synergism stays relatively constant in these cases. Cu alone contributes just 6% of total •OH in the high case, whereas Fe/Cu synergism contributes 36%; therefore Cu is still important for total •OH production even though there is a plateau in the contribution from Cu individually.

Comparison with Other Measures of Oxidative Potential. In this and past work we systematically identified the responses from soluble transition metals and quinones (both individually and in mixtures) in three cell-free assays for ROS: •OH formation (this work), HOOH formation,[22] and dithiothreitol (DTT) loss.[17] In Figure 7 we show the relative contribution of each species to the total assay response for a hypothetical PM sample containing the median concentrations reported in the literature (Supporting Information Table S2).

For this median composition, soluble Cu accounts for a significant fraction of oxidant production in all three assays: 54% of DTT loss, 96% of HOOH production, and 36% of •OH production (as well as an additional 32% of •OH via synergy with Fe). Fe is only important in •OH production, but can also suppress HOOH, as we discussed above. Quinones contribute little to HOOH or •OH formation, but PQN accounts for a significant fraction of DTT loss. Additionally, Mn contributes a quarter to DTT loss but does not contribute to HOOH or •OH production.

There is one clear message from Figure 7: soluble Cu likely plays a key role in the acellular generation of ROS and oxidative stress by inhaled atmospheric particles, based on its major role in all three assays. This is consistent with previous studies of copper toxicity: (1) in vitro cellular assays show the Cu particles (especially nanoparticles) are remarkably toxic, likely because of ROS generation,[41−43] (2) in vivo animal studies generally show that inhaled and instilled particulate and soluble Cu cause adverse effects,[44−46] and (3) epidemiological studies reveal an association of ambient particulate Cu with adverse health effects and mortality in humans.[47,48] Cu is known to be toxic, and is commonly used as a fungicide, pesticide, and preservative.[49,50] Despite this, there is currently little regulation of airborne Cu, which is not considered a hazardous air pollutant (HAP) by the U.S. Environmental Protection Agency. While copper is considered a toxic air contaminant (TAC) by the California EPA, the particulate Cu chronic standard (reference exposure level or REL) set by the California Office of Environmental Health Hazard Assessment (OEHHA) is 100 $\mu g/m^3$.[51] Ambient concentrations of Cu are low (0.001−0.050 $\mu g/m^3$)[52] but Cu dominates direct ROS production in our assays, indicating that further consideration of the potential toxicity of particulate Cu is necessary. Additionally, in all three cell-free assays, Cu exhibits a nonlinear concentration−response curve, which could mask the effect of Cu when using correlation analysis or even in epidemiological studies. Finally, as we describe in section S5 of the Supporting Information, ROS production from Cu in cell-free assays may be confounded by high background concentrations of Cu in the salts used in the assay if Chelex treatment is not applied.

DOI: 10.1021/acs.est.5b01606
Environ. Sci. Technol. 2015, 49, 9317−9325

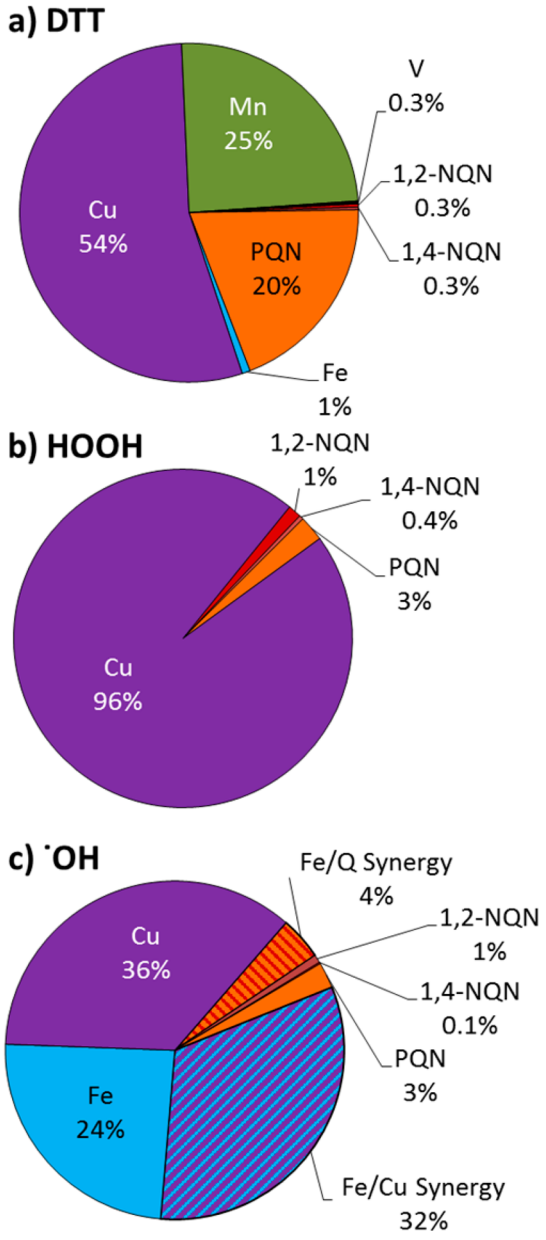

Figure 7. Relative contributions of redox-active species to a) DTT loss,[17] b) HOOH production,[22] and c) •OH production (this work) using the median particulate concentrations of ambient quinones and soluble metals reported in the literature (Supporting Information Table S2).

■ ASSOCIATED CONTENT

Supporting Information

Supporting material, consisting of six sections, four figures, and two tables. The Supporting Information is available free of charge on the ACS Publications website at DOI: 10.1021/acs.est.5b01606.

■ AUTHOR INFORMATION

Corresponding Author

*Phone (530) 754-6095; fax: (530) 752-1552; e-mail: canastasio@ucdavis.edu.

Notes

The authors declare no competing financial interest.

■ ACKNOWLEDGMENTS

We thank Tobias Kraft and Alexander McFall for laboratory assistance, Ralph Propper (CARB) for input, and an anonymous reviewer for insightful comments. Funding for this project was provided by the California Air Resources Board (agreement number 18467), by the National Institute of Environmental Health Sciences (NIEHS) (grant number P42ES004699), by an EPA STAR Graduate Fellowship to JC (FP-917181) and by the California Agricultural Experiment Station (Project CA-D-LAW-6403-RR). The statements and conclusions in this report are those of the authors and not necessarily those of the California Air Resources Board or the U.S. EPA. This publication has not been formally reviewed by ARB, EPA, NIEHS, or NIH. The mention of commercial products, their source, or their use in connection with material reported herein is not to be construed as actual or implied endorsement of such products.

■ REFERENCES

(1) Dockery, D. W.; Pope, C. A.; Xu, X. P.; Spengler, J. D.; Ware, J. H.; Fay, M. E.; Ferris, B. G.; Speizer, F. E. An association between air pollution and mortality in 6 United-States cities. *N. Engl. J. Med.* **1993**, *329* (24), 1753−1759.

(2) Ito, K.; Mathes, R.; Ross, Z.; Nadas, A.; Thurston, G.; Matte, T. Fine particulate matter constituents associated with cardiovascular hospitalizations and mortality in New York City. *Environ. Health Perspect.* **2010**, *119* (4), 467−473.

(3) Li, X. Y.; Gilmour, P. S.; Donaldson, K.; MacNee, W. Free radical activity and pro-inflammatory effects of particulate air pollution (PM(10)) in vivo and in vitro. *Thorax* **1996**, *51* (12), 1216−1222.

(4) Dellinger, B.; Pryor, W. A.; Cueto, R.; Squadrito, G. L.; Hedge, V.; Deutsch, W. A. Role of free radicals in the toxicity of airborne fine particulate matter. *Chem. Res. Toxicol.* **2001**, *14* (10), 1371−1377.

(5) Li, N.; Xia, T.; Nel, A. E. The role of oxidative stress in ambient particulate matter-induced lung diseases and its implications in the toxicity of engineered nanoparticles. *Free Radical Biol. Med.* **2008**, *44* (9), 1689−1699.

(6) Campen, M. J.; Nolan, J. P.; Schladweiler, M. C. J.; Kodavanti, U. P.; Costa, D. L.; Watkinson, W. P. Cardiac and thermoregulatory effects of instilled particulate matter-associated transition metals in healthy and cardiopulmonary-compromised rats. *J. Toxicol. Environ. Health, Part A* **2002**, *65* (20), 1615−1631.

(7) Halliwell, B. Antioxidant characterization - methodology and mechanism. *Biochem. Pharmacol.* **1995**, *49* (10), 1341−1348.

(8) Risom, L.; Møller, P.; Loft, S. Oxidative stress-induced DNA damage by particulate air pollution. *Mutat. Res., Fundam. Mol. Mech. Mutagen.* **2005**, *592*, 119−137.

(9) Keeling, B.; Li, K. Y.; Churg, A. Iron Enhances Uptake of Mineral Particles and Increases Lipid-Peroxidation in Tracheal Epithelial-Cells. *Am. J. Respir. Cell Mol. Biol.* **1994**, *10* (6), 683−688.

(10) Aust, A. E.; Eveleigh, J. F. Mechanisms of DNA oxidation. *Proc. Soc. Exp. Biol. Med.* **1999**, *222* (3), 246−252.

(11) van Maanen, J. M. S.; Borm, P.; Knaapen, A.; van Herwijnen, M.; Schilderman, P. A. E. L.; Smith, K. R.; Aust, A. E.; Tomatis, M.; Fubini, B. In vitro effects of coal fly ashes: Hydroxyl radical generation, iron release, and DNA damage and toxicity in rat lung epithelial cells. *Inhalation Toxicol.* **1999**, *11*, 1123−1141.

(12) Halliwell, B.; Cross, C. E. Oxygen-derived species - their relation to human-disease and environmental stress. *Environ. Health Perspect.* **1994**, *102*, 5−12.

(13) Goldstein, S.; Meyerstein, D.; Czapski, G. The Fenton reagents. *Free Radical Biol. Med.* **1993**, *15* (4), 435−445.

(14) Valavanidis, A.; Vlahoyianni, T.; Fiotakis, K. Comparative study of the formation of oxidative damage marker 8-hydroxy-2 ′-deoxy-guanosine (8-OHdG) adduct from the nucleoside 2 ′-deoxyguanosine by transition metals and suspensions of particulate matter in relation to

DOI: 10.1021/acs.est.5b01606
Environ. Sci. Technol. 2015, 49, 9317−9325

metal content and redox reactivity. *Free Radical Res.* **2005**, *39* (10), 1071−1081.
(15) Lloyd, D. R.; Phillips, D. H. Oxidative DNA damage mediated by copper(II), iron(II) and nickel(II) Fenton reactions: evidence for site-specific mechanisms in the formation of double-strand breaks, 8-hydroxydeoxyguanosine and putative intrastrand cross-links. *Mutat. Res., Fundam. Mol. Mech. Mutagen.* **1999**, *424* (1−2), 23−36.
(16) Ball, J. C.; Straccia, A. M.; Young, W. C.; Aust, A. E. The formation of reactive oxygen species catalyzed by neutral, aqueous extracts of NIST ambient particulate matter and diesel engine particles. *J. Air Waste Manage. Assoc.* **2000**, *50* (11), 1897−1903.
(17) Charrier, J. G.; Anastasio, C. On dithiothreitol (DTT) as a measure of oxidative potential for ambient particles: evidence for the importance of soluble transition metals. *Atmos. Chem. Phys.* **2012**, *12*, 9321−9333.
(18) Fischer, H. Mechanisms and function of DUOX in epithelia of the lung. *Antioxid. Redox Signaling* **2009**, *11* (10), 2453−2465.
(19) Charrier, J. G.; Anastasio, C. Impacts of antioxidants on hydroxyl radical production from individual and mixed transition metals in a surrogate lung fluid. *Atmos. Environ.* **2011**, *45* (40), 7555−7562.
(20) DiStefano, E.; Eiguren-Fernandez, A.; Delfino, R. J.; Sioutas, C.; Froines, J. R.; Cho, A. K. Determination of metal-based hydroxyl radical generating capacity of ambient and diesel exhaust particles. *Inhalation Toxicol.* **2009**, *21* (8−11), 731−738.
(21) Vidrio, E.; Jung, H.; Anastasio, C. Generation of hydroxyl radicals from dissolved transition metals in surrogate lung fluid solutions. *Atmos. Environ.* **2008**, *42*, 4369−4379.
(22) Charrier, J. G.; Mcfall, A. S.; Richards-Henderson, N. K.; Anastasio, C. Hydrogen peroxide formation in a surrogate lung fluid by transition metals and quinones present in particulate matter. *Environ. Sci. Technol.* **2014**, *48* (12), 7010−7017.
(23) Chung, M. Y.; Lazaro, R. A.; Lim, D.; Jackson, J.; Lyon, J.; Rendulic, D.; Hasson, A. S. Aerosol-borne quinones and reactive oxygen species generation by particulate matter extracts. *Environ. Sci. Technol.* **2006**, *40* (16), 4880−4886.
(24) Valavanidis, A.; Fiotakis, K.; Bakeas, E.; Vlahogianni, T. Electron paramagnetic resonance study of the generation of reactive oxygen species catalysed by transition metals and quinoid redox cycling by inhalable ambient particulate matter. *Redox Rep.* **2005**, *10* (1), 37−51.
(25) Prousek, J.; Palackova, E.; Priesolova, S. A.; Markova, L.; Alevova, A. Fenton- and fenton-like AOPs for wastewater treatment: From Laboratory-to-plant-scale application. *Sep. Sci. Technol.* **2007**, *42* (7), 1505−1520.
(26) Shang, Y.; Chen, C.; Li, Y.; Zhao, J.; Zhu, T. Hydroxyl radical generation mechansim during the redox cycling process of 1,4-naphthoquinone. *Environ. Sci. Technol.* **2012**, *46* (5), 2935−2942.
(27) Li, Y.; Zhu, T.; Zhao, J.; Xu, B. Interactive enhancements of ascorbic acid and iron in hydroxyl radical generation in quinone redox cycling. *Environ. Sci. Technol.* **2012**, *46* (18), 10302−10309.
(28) Shen, H.; Anastasio, C. A comparison of hydroxyl radical and hydrogen peroxide generation in ambient particle extracts and laboratory metal solutions. *Atmos. Environ.* **2012**, *46*, 665−668.
(29) Shen, H.; Anastasio, C. Formation of hydroxyl radical from San Joaquin Valley particles extracted in a cell-free surrogate lung fluid. *Atmos. Chem. Phys.* **2011**, *11* (18), 9671−9682.
(30) Vidrio, E.; Phuah, C. H.; Dillner, A. M.; Anastasio, C. Generation of hydroxyl radicals from ambient fine particles in a surrogate lung fluid solution. *Environ. Sci. Technol.* **2009**, *43* (3), 922−927.
(31) Costa, D. L.; Dreher, K. L. Bioavailable transition metals in particulate matter mediate cardiopulmonary injury in healthy and compromised animal models. *Environ. Health Perspect.* **1997**, *105*, 1053−1060.
(32) Gavett, S. H.; Madison, S. L.; Dreher, K. L.; Winsett, D. W.; McGee, J. K.; Costa, D. L. Metal and sulfate composition of residual oil fly ash determines airway hyperreactivity and lung injury in rats. *Environ. Res.* **1997**, *72* (2), 162−172.
(33) Dreher, K. L.; Jaskot, R. H.; Lehmann, J. R.; Richards, J. H.; McGee, J. K.; Ghio, A. J.; Costa, D. L. Soluble transition metals mediate residual oil fly ash induced acute lung injury. *J. Toxicol. Environ. Health* **1997**, *50* (3), 285−305.
(34) Antonini, J. M.; Taylor, M. D.; Leonard, S. S.; Lawryk, N. J.; Shi, X. L.; Clarke, R. W.; Roberts, J. R. *Mol. Cell. Biochem.* **2004**, *255*, 257−265.
(35) Aust, A. E.; Ball, J. C.; Hu, A. A.; Lighty, J. S.; Smith, K. R.; Straccia, A. M.; Veranth, J. M.; Young, W. C. *Particle Characteristics Responsible for Effects on Human Lung Epithelial Cells*, Research Report; Health Effects Institute, 2002; Vol. *110*, pp 1−65, discussion 67−76.
(36) Richards-Henderson, N. K.; Charrier, J. G.; Bein, K. J.; Bau, D.; Wexler, A. S.; Anastasio, C. Oxidant production from source-oriented particulate matter − Part 2: Hydrogen peroxide and hydroxyl radical. *Atmos. Chem. Phys.* **2015**, *15*, 2327.
(37) Jung, H.; Guo, B.; Anastasio, C.; Kennedy, I. M. Quantitative measurements of the generation of hydroxyl radicals by soot particles in a surrogate lung fluid. *Atmos. Environ.* **2006**, *40* (6), 1043−1052.
(38) Kachur, A. V.; Held, K. D.; Koch, C. J.; Biaglow, J. E. Mechanism of production of hydroxyl radicals in the copper-catalyzed oxidation of dithiothreitol. *Radiat. Res.* **1997**, *147* (4), 409−415.
(39) Team, R. D. C. R Development Core Team. *R: A Language and Environment for Statistical Computing*. R Foundation for Statistical Computing, Vienna, Austria, 2008; http://www.r-project.org/.
(40) Lin, P.; Yu, J. Z. Generation of reactive oxygen species mediated by humic-like substances in atmospheric aerosols. *Environ. Sci. Technol.* **2011**, *45* (24), 10362−10368.
(41) Karlsson, H. L.; Cronholm, P.; Hedberg, Y.; Tornberg, M.; De Battice, L.; Svedhem, S.; Wallirider, I. O. Cell membrane damage and protein interaction induced by copper containing nanoparticles - Importance of metal release process. *Toxicology* **2013**, *313* (1), 59−69.
(42) Fahmy, B.; Cormier, S. A. Copper oxide nanoparticles induce oxidative stress and cytotoxicity in airway epithelial cells. *Toxicol. In Vitro* **2009**, *23* (7), 1365−1371.
(43) Jing, X.; Park, J. H.; Peters, T. M.; Thorne, P. S. Toxicity of copper oxide nanoparticles in lung epithelial cells exposed to air-liquid interface compared with in vivo assessment. *Toxicol. In Vitro* **2015**, *29* (3), 502−511.
(44) Dye, J. A.; Lehmann, J.; McGee, J.; Winsett, D. W.; Ledbetter, A.; Everitt, J.; Ghio, A. J.; Costa, D. L., Acute pulmonary toxicity of particulate matter filter extracts in rats: Coherence with epidemiologic sutides in Utah valley residents. *Environ. Health Perspect.* **2001**, *109*, (395−403).39510.2307/3434787
(45) Rice, T.; Clarke, R. W.; Godleski, J. J.; Al-Mutairi, E.; Jiang, N.; Hauser, R.; Paulauskis, J. Differential ability of transition metals to induce pulmonary inflammation. *Toxicol. Appl. Pharmacol.* **2001**, *177* (1), 46−53.
(46) Pettibone, J.; Adamcakova-Dodd, A.; Thorne, P.; O'Shaughnessy, P.; Weydert, J.; Grassian, V. Inflammatory response of mice following inhalation exposure to iron and copper nanoparticles. *Nanotoxicology* **2008**, *2* (4), 189−204.
(47) Ostro, B.; Feng, W.-Y.; Broadwin, R.; Green, S.; Lipsett, M. The effects of components of fine particulate air pollution on mortality in California: Results from CALFINE. *Environ. Health Perspect.* **2006**, *115* (1), 13−19.
(48) Ostro, B.; Hu, J.; Goldberg, D.; Reynolds, P.; Hertz, A.; Bernstein, L.; Kleeman, M. J. Associations of mortality with long-term eposures to fine and ultrafine particles, species and sources: results from the California teachers study cohort. *Environ. Health Perspect.* **2015**, *117* (3), 549−556.
(49) Brun, L. A.; Maillet, J.; Richarte, J.; Herrmann, P.; Remy, J. C. Relationships between extractable copper, soil properties and copper uptake by wild plants in vineyard soils. *Environ. Pollut.* **1998**, *102* (2), 151−161.
(50) Freeman, M. H.; McIntyre, C. R. Copper-based wood preservatives. *For. Prod. J.* **2008**, *58* (11), 7.
(51) OEHHA, Appendix D. Individual acute, 8-h, and chronic reference exposure level summaries, 2008. http://oehha.ca.gov/air/hot_spots/2008/AppendixD1_final.pdf#page=170.

DOI: 10.1021/acs.est.5b01606
Environ. Sci. Technol. 2015, 49, 9317−9325

(52) Herner, J. D.; Green, P. G.; Kleeman, M. J. Measuring the trace elemental composition of size-resolved airborne particles. *Environ. Sci. Technol.* **2006**, *40* (6), 1925−1933.

DOI: 10.1021/acs.est.5b01606
Environ. Sci. Technol. 2015, 49, 9317−9325